Laser-Control of Ferro- and Antiferromagnetism

M. Trzeciecki[1,2], O. Ney[1], G. P. Zhang[3], and W. Hübner[1]

[1] Max-Planck-Institut für Mikrostrukturphysik, Weinberg 2, D-06120 Halle, Germany
[2] Institute of Physics, Warsaw University of Technology, Koszykowa 75, PL 00-662 Warsaw, Poland
[3] Dept. of Physics and Astronomy, University of Tennessee, Knoxville, Tennessee 37996-1200, USA

Abstract. We set up the theory of ultrafast spin dynamics in the ferromagnetic Ni and antiferromagnetic NiO. Investigating the speed limits of spin dynamics is of a very high importance for future computer memory designs, such as Magnetic Random Access Memories. We find magnetic dephasing in Ni and dephasing-rephasing processes in NiO on the femtosecond timescales. Thus, NiO presents a very interesting feature of fast spin dynamics accompanied by a long lasting (till nanoseconds) coherence, which may find applications e.g. in quantum computing. These effects can be probed e.g. by nonlinear magneto-optical methods such as Second Harmonic Generation (SHG). Additionally, we demonstrate a laser-driven remagnetization in Ni, which is the first step towards spin control.

The current speed of magnetic recording is of the order of nanoseconds, i.e. close to a single precession cycle of the magnetization (Larmor frequency). Achieving a higher speed will require completely new approaches, such as hybrid or optical recording. In order to overcome the deficiences of the contemporary computer memories, both permanent and dynamic, new designs like magnetic random access memories (MRAMs) are under development [1]. They will eliminate the mechanical motion and the hierarchical structure of the contemporary memories and simplify the design of the CPUs. One of the most important components of these MRAMs are tunneling magnetoresistance (TMR) devices, where the read-out current passing through the device depends on the relative magnetization of two ferromagnetic layers. The central layer of this trilayer structure consists of an oxide sandwiched between a soft and a hard magnetic layer. Therefore, the performance of these future devices depends heavily on the properties of oxides, which may be nonmagnetic or antiferromagnetic. Antiferromagnets are necessary for the exchange-bias junctions, which find applications such as TMR structures. Therefore, the investigation of magnetic dynamics in ferromagnetic metals as well as antiferromagnetic (AF) oxides is of basic scientific and technological relevance. The simple structures of cubic AF oxides and their pronounced symmetry properties (otherwise encountered in molecules rather than condensed matter) make them a very interesting object of investigation. A useful investigation

method for these materials is optical Second Harmonic Generation (SHG), since it has been proven sensitive to *bulk* antiferromagnetism [2]. Also, the SHG signal is sensitive to symmetry properties. Moreover, in an SHG experiment a whole array of parameters can easily be varied, which facilitates *dynamical*, i.e. time-resolved experiments. In these experiments (pump-and-SHG-probe experiments), magnetization at femtosecond time scales has been measured for metals. In our work, we address this sensitivity to femtosecond magnetism from the theoretical point of view, both for ferromagnetic metals and for antiferromagnetic metal oxides.

In contemporary computer memories (permanent and RAM) the speed limit is put by thermally and magnetically driven demagnetization that occurs on a nanosecond time scale. This time scale is basically set by the spin-lattice, magnetic dipole, and Zeeman interactions and has long been considered as a speed limit also for magneto-optical technology. However, this limit is challenged by recent experimental observations [3–6]. These short time scales of the observed spin dynamics promoted the development of appropriate theoretical models, since the spin-lattice relaxation processes that occur at the time scales of several tens to hundreds of picoseconds [7] cannot be responsible for the observed effects. The concept of different temperatures (charge, spin, and lattice temperature) frequently used for large, separated time scales and originally invoked to explain also these results [3,4] is not strictly valid, since at so short time scales it is impossible to define a temperature, which is rather an equilibrium property. A proper model, dephasing of complex excited-state populations, has been developed by us for both linear [8,9] and nonlinear [9–11] magneto-optics from ferromagnets and antiferromagnets. Here, we present the theoretical investigation of laser-induced demagnetization in *ferromagnetic* Ni [12], and the investigation of the time-dependent *antiferromagnetism* in NiO, addressing typical pump-probe laser experiments.

In a pump-probe experiment, the first (strong) laser pulse is used to excite the material. The magnetic dynamics of this material can be subsequently probed by a probe pulse, that arrives at a variable time delay. The response of the sample to this second pulse can be analyzed e.g. at the same or twice the fundamental probe frequency. The latter process (pump-and-SHG-probe experiment) is particularly suited for probing *surface* ferro- and antiferromagnetism on femtosecond time scales [10,13,14].

Figure 1(a) schematically presents the many-body levels of a Ni atom in Ni and NiO. The ground state triplet is the one of large spin, and excitation from this state into high-lying low-spin states leads to a reduction of the magnetic moment. Our results for the *ferromagnetic* Ni monolayer show a drop of the magnetization within the first femtoseconds after an excitation (Fig. 1(b), pulse P_1). This magnetization drop becomes larger with increasing intensity I of the pump pulse, in agreement with experiments [4]. The magnetization drop results from the fact that spin-orbit coupling (SOC) mixes the

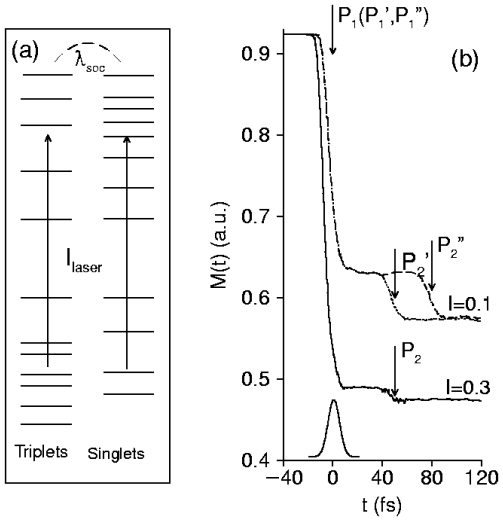

Fig. 1. (a) Many-body level scheme of Ni and NiO. For the sake of clarity, the triplets and singlets are displaced horizontally. (b) Magnetization drop at various pump pulse intensities I. The laser pulse profile is shown as well [12]

character of triplet and singlet states in Ni, while the laser field uses this as an avenue to demagnetize the ferromagnetic material. Thus, this novel effect is a cooperative effect of SOC and the laser field. The drop of magnetization can be followed by a linear magneto-optical method or SHG and occurs on the ultrafast timescale of less than 40 femtoseconds. Thus it supersedes the speed limit of conventional magnetic recording by four orders of magnitude.

Importantly, such a demagnetization can be tuned, e.g. by the variation of laser intensity or pump-pulse sequence (2 pump pulses P_1 and P_2), which is indispensable to applications such as ultrafast control of magneto-optical gating. By intensity variations, the drop of magnetization can be manipulated; by different delays one can inscribe the information within different time intervals. By use of appropriate parameters of the optical pulse, it is even possible to restore the magnetization partially (Fig. 2). A combination of these possibilities yields a large flexibility to control spin.

As stated before, SHG has the unique potential to become a tool for investigating *oxide interfaces* (even buried ones), where other techniques fail. Until very recently, it has been proven to be a very useful technique for the investigation of ferromagnetism at surfaces. The obvious question is if this technique can also yield some new information in the case of more general spin configurations, such as antiferromagnetic (AF) ordering at interfaces. An experimental answer to this question has been provided by Fiebig *et al.* [2,15], who obtained a pronounced optical contrast from AF 180° domains of

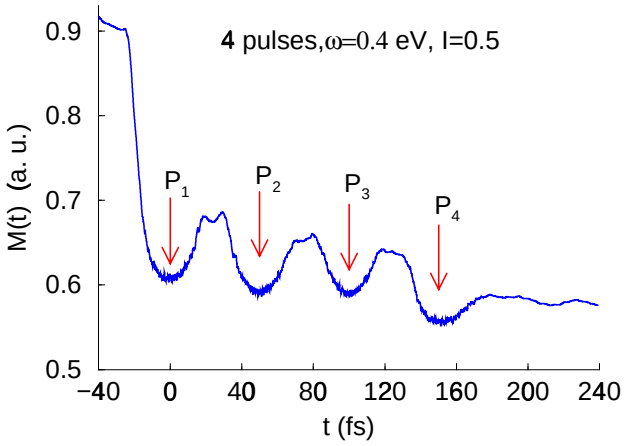

Fig. 2. Two-bit controlled remagnetization in Ni

rhombohedral bulk Cr_2O_3. Since it is known that, in *cubic* materials, within the electric-dipole approximation, optical SHG originates only from surfaces, interfaces, or thin films, an important question is if SHG is also sensitive to antiferromagnetism at surfaces of cubic antiferromagnets. This question was answered by symmetry analysis, which also lays the ground for the theoretical investigation of antiferromagnetism on femtosecond timescales.

The symmetry analysis addresses the nonlinear magnetooptical susceptibility tensor $\chi^{(2\omega)}$, which is the source of SHG within the electric-dipole approximation. In our work we addressed various antiferromagnetic spin structures on low index surfaces of cubic antiferromagnets, among them all structures which are possible for NiO [13,14]. As the result of the group-theoretical analysis we obtain non-vanishing elements of the $\chi^{(2\omega)}$ tensor. These findings demonstrate the possibility to distinguish the antiferromagnetic surfaces of cubic crystals from ferromagnetic and paramagnetic surfaces. Such a distinction can be performed in an experiment where the polarization of the incident and outgoing (i.e. SHG) light beams can be varied. Moreover, we predict the possibility of antiferromagnetic surface *domain imaging* by SHG. Besides these technologically important results, we addressed the issue of *time-reversal operation* in nonlinear magneto-optics [16]. The result, inconsistence of time reversal and magnetization reversal operations, has a deep meaning for the basic scientific understanding of magnetooptics.

This problem is connected in an interesting way to the issue of magnetic anisotropy in crystals [19]. Anisotropy energy is degenerate under time reversal, since the easy axis is bidirectional. On the other hand, magneto-optical effects change sign when time (or magnetization) reversal is applied.

The main deficiency of the abovementioned symmetry analysis is the lack of quantitative predictions. For that purpose, we developed an electronic

theory for the nonlinear magneto-optics on NiO (001), based upon the results of our symmetry analysis and using the previously described framework for Ni. Taking into account the electronic configurations $3d^8$, $3d^7$, and $3d^6$ of the Ni ion opens the way to describe properly not only the highly excited states of NiO, but also other materials. With only slight modification of this work, nearly all elements of the periodic table can be addressed, which overcomes the earlier limitations of that theory. Especially, the extension to other cubic metal oxides such as CoO or FeO is straightforward. Our ligand-field-theory approach allows us to fully consider the *surface* of the material. We are not restricted to a monolayer of NiO.

In antiferromagnetic NiO, the electronic states couple to form many-body states (rather than bands as in the case of Ni) [11]. First we determine the two-, three-, and four-body wavefunctions which describe the excited states of a Ni^{++} ion. These functions form a basis for our Hamiltonian, which exhibits a full spherical symmetry. Next we introduce a ligand field to reduce the symmetry to cubic (bulk material) and square (crystal surface). We fit the ligand-field parameters to the experimental energy values. Then the Hamiltonian describes excited states at the NiO (001) surface and allows for obtaining the nonlinear spectrum of the material. The results show that the nonvanishing tensor elements are proportional to the antiferromagnetic order parameter.

Here, we present the spectra of two tensor elements: the prototypic paramagnetic tensor element $\chi^{(2\omega)}_{zzz}$ and the prototypic AF tensor element $\chi^{(2\omega)}_{zxy}$ in Fig. 3. In both spectra, all the features fall within the fundamental gap of bulk NiO, which we assume to be at 4.0 eV. The dominant structure in both spectra corresponds to the transitions from the ground state to the states resulting from the split ^{3}P state, which are all located near 3.0 eV, see Tab. 1. The position of the peak around 1.5 eV corresponds to the fact that the tensor describes SHG. Other, smaller peaks related to transitions between various states are also present. Another feature of the calculated spectra is that the tensor elements are complex and their phases vary. This has important consequences for the AF domain imaging using SHG, as discussed in [16].

The main distinctive feature of the spectrum of the AF tensor element $\chi^{(2\omega)}_{zxy}$ are additional peaks due to transitions allowed by antiferromagnetic symmetry breaking. The lines above 1.5 eV are completely absent in the spectrum of the paramagnetic tensor element $\chi^{(2\omega)}_{zxy}$, since transitions of higher energy would involve singlet states (which are the only states above 3.0 eV). The effect of mixing in the singlet states is, however, much more pronounced in the AF tensor element than in the paramagnetic one, due to the spin-orbit coupling. Consequently, there are several spectral lines which have an "antiferromagnetic" character, we expect them to be suitable for antiferromagnetic spin dynamics. Note that the AF SHG tensor element $\chi^{(2\omega)}_{zxy}$ is *linear* in the AF order parameter. Another interesting result is that both tensor elements

Table 1. States at the (001) surface of NiO. The ligand field parameter ε_0 describes the energy shift in the crystal field, D_q is the level splitting in the cubic O_h environment, D_S and D_U correspond to the level splitting in the octahedral O and C_{4v} symmetries, respectively

free-ion state	surface state	ligand-field correction	energy [eV]
^{1}S	^{1}A$_1$	$2\varepsilon_0$	8.6940
^{3}P	^{3}A$_1$	$2\varepsilon_0 + \frac{14}{5}D_S$	2.9719
	^{3}E	$2\varepsilon_0 - \frac{7}{5}D_S$	3.0081
^{1}D	^{1}A$_1$	$2\varepsilon_0 + \frac{6}{7}D_S + \frac{24}{7}D_q$	2.7519
	^{1}B$_1$	$2\varepsilon_0 - \frac{6}{7}D_S + \frac{24}{7}D_q + \frac{20}{7}D_U$	2.6531
	^{1}B$_2$	$2\varepsilon_0 - \frac{6}{7}D_S - \frac{16}{7}D_q - \frac{20}{7}D_U$	3.2281
	^{1}E	$2\varepsilon_0 - \frac{3}{7}D_S - \frac{16}{7}D_q$	3.1036
^{3}F	^{3}B$_1$	$2\varepsilon_0 + 2D_q - 5D_U$	0.0000
	^{3}E	$2\varepsilon_0 - D_S + 2D_q + \frac{15}{4}D_U$	1.4370
	^{3}B$_2$	$2\varepsilon_0 + 12D_q + 5D_U$	1.0027
	^{3}A$_2$	$2\varepsilon_0 - \frac{4}{5}D_S - 6D_q$	1.2985
	^{3}E	$2\varepsilon_0 + \frac{2}{5}D_S - 6D_q - \frac{15}{4}D_U$	0.6553
^{1}G	^{1}A$_{1\alpha}$	$2\varepsilon_0 + 4D_q + \frac{5}{3}D_U$	3.9556
	^{1}A$_{1\beta}$	$2\varepsilon_0 + \frac{8}{7}D_S + \frac{4}{7}D_q - \frac{5}{3}D_U$	3.5888
	^{1}B$_1$	$2\varepsilon_0 - \frac{8}{7}D_S + \frac{4}{7}D_q + \frac{15}{7}D_U$	4.2553
	^{1}A$_2$	$2\varepsilon_0 + 4D_S + 2D_q$	3.8240
	^{1}E	$2\varepsilon_0 - 2D_S + 2D_q + \frac{5}{4}D_U$	4.2051
	^{1}B$_2$	$2\varepsilon_0 - \frac{8}{7}D_S - \frac{26}{7}D_q - \frac{15}{7}D_U$	3.7777
	^{1}E	$2\varepsilon_0 + \frac{4}{7}D_S - \frac{26}{7}D_q - \frac{5}{4}D_U$	3.7798

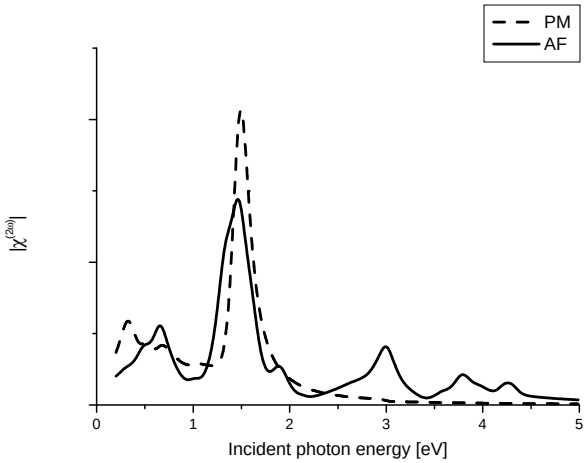

Fig. 3. Spectrum of the paramagnetic tensor element $\chi^{(2\omega)}_{zzz}$ (dashed) and the antiferromagnetic tensor element $\chi^{(2\omega)}_{zyx}$ (full)

are of similar magnitude. This is a favorable condition for AF domain imaging. Taking into account the magnitudes of both tensor elements presented in this section, the domain contrast should be as large as in ferromagnets (where it is of the order of *unity* in SHG, as opposed to the small domain contrast in MOKE). This large contrast provides a large driving force for the dynamics of the nonlinear magneto-optical response.

Next, we turn to the calculation of the AF spin dynamics on the femtosecond time scale. The initial excitation is assumed to be infinitesimally short in time (the excitation pulse is already completed when our dynamics starts) but its energy distribution follows a Gaussian profile, centered at 2 eV and 20 eV wide (truncated at 0 eV, so that no negative energies appear). This width of the excitation allows us to probe the fast limit of the dynamics, since all the energy levels (including the highest) are populated and consequently all de-excitation channels are open. Restricting the Hamiltonian to electronic on-site interactions complies with this limit. The initial excitation causes a strong redistribution of charges among the energy levels, visible as a drop [17] of the observed signal compared to its value in a static experiment. The time

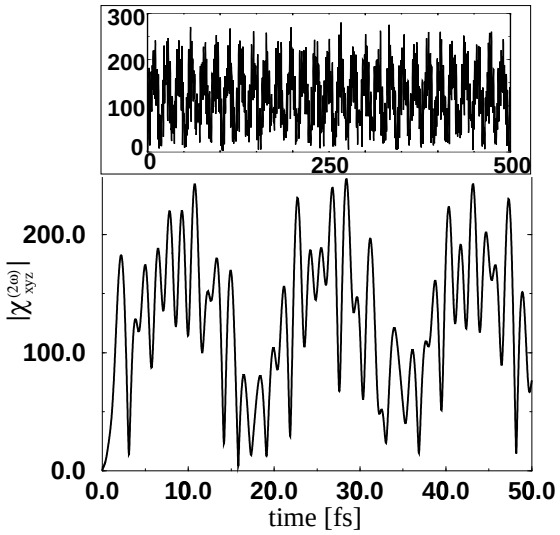

Fig. 4. Time evolution of the tensor element $\chi^{(2\omega)}_{zyx}$ within the first 50 fs after the excitation. The inset shows the evolution of the same tensor element within the first 500 fs. The units are the same as in Fig. 3

evolution of the excited system then results from the quantum phase factors and has no classical analogue. Fig. 4 shows the calculated dynamics of the AF tensor element $\chi^{(2\omega)}_{xyz}(t)$ within the first 500 fs at the fundamental photon energy 0.55 eV. Such a dynamics can be probed in an interferometric SHG

experiment. We find that there is no decay of the envelope of $\chi^{(2\omega)}_{xyz}(t)$, unlike for metallic systems [10]. The coherence is preserved for a long time (until phenomena neglected within this framework take place, like electron-phonon coupling), which manifests itself by beats of constant amplitude repeated regularly every 20 fs (Fig. 4). Consequently, we predict spin coherence times in magnetic oxides that are four orders of magnitude longer than the ultimate speed of the spin and charge dynamics. This allows for many read-write cycles during the intrinsic life-time of the excitation. Besides, it fulfills one of the important conditions for quantum information [18]. This finding is in line with the experimentally determined widths of spectral lines in oxides [15] (tens of μeV, which corresponds to tens of picoseconds coherence times), and shows the potential of magnetic oxide interfaces for various technological applications on ultrafast time scales, such as novel computer memories and quantum computing.

	theory	experiment
Ni (FM)		
laser pulse	δ (0 fs)	20 fs
dephasing	5 - 10 fs	20 fs
laser pulse	10 fs	20 fs
demagnetization	20 - 40 fs	80 fs
NiO (AF)		
laser pulse	δ (0 fs)	$\sim$ 100 fs
de- and rephasing	20 fs	$<$ 100 fs
laser pulse	δ (0 fs)	$\sim$ 100 fs
decoherence	∞ ($>$ 1ps)	$\sim$ 1 ns

Table 2. Comparison of our predictions with the experimental findings

Now, let us compare the achievements of our theory for both Ni and NiO with the experimental results (see Tab. 2). As described here, the theory for metallic Ni is more advanced than the model for NiO, nevertheless for both materials we use pump pulses which have a delta-function shape in time. Obviously, the experimental lasers issue pulses of a finite duration. The dephasing speed (for NiO we call it dephasing and rephasing) agree very well in the order of magnitude, further experiments may even improve this agreement as higher time resolution is achieved. The progress in the theoretical description of laser induced transitions in Ni made it possible to mimic a 10 fs probe pulse, while in an experiment 20 fs has been achieved. Consequently, the experimental demagnetization speed in Ni agrees to a factor of two with the speed predicted by us. The decoherence in NiO is predicted to be caused by phonons and thus takes place within nanoseconds. The experimental result of the coherence times of 1 ns corresponds to our prediction. Thus, our theory yields the important finding that there is no physical speed

limit for magnetic recording devices in the nanosecond regime. It possible to manipulate spins optically on times as short as femtoseconds.

We acknowledge the financial support of the European networks NOMOKE (contract number FMRX-CT96-0015), Dynaspin (contract number ERBFMRX-CT97-0124), and the DFG Forschergruppe "Oxydische Grenzflächen".

References

1. J. de Boeck and G. Borghs, Phys. World, April 1999, 27 (1999).
2. M. Fiebig, D. Fröhlich, and G. Sluyterman v. L., Appl. Phys. Lett. **66**, 2906 (1995)
3. E. Beaurepaire, J.-C. Merle, A. Daunois, and J.-Y. Bigot, Phys. Rev. Lett. **76**, 4250 (1996)
4. J. Hohlfeld, E. Matthias, R. Knorren, and K. H. Bennemann, Phys. Rev. Lett. **78**, 4861 (1997), *ibid* **79**, 960 (1997) (erratum)
5. A. Scholl, L. Baumgarten, R. Jacquemin, and W. Eberhardt, Phys. Rev. Lett. **79**, 5146 (1997)
6. M. Aeschlimann, M. Bauer, S.Pawlik, W. Weber, R. Burgermeister, D.Oberli, and H. C. Siegmann, Phys. Rev. Lett. **79**, 5158 (1997)
7. A. Vaterlaus, T. Beutler, and F. Meier, Phys. Rev. Lett. **67**, 3314 (1991)
8. W. Hübner and G. P. Zhang, Phys. Rev. B **58**, R5920 (1998)
9. W. Hübner and G. P. Zhang, J. Magn. Magn. Matt. **189**, 101 (1998)
10. G. P. Zhang and W. Hübner, Appl. Phys. B **68**, 495 (1999)
11. M. Trzeciecki, "Second Harmonic Generation from Antiferromagnetic Interfaces", PhD Thesis, Martin-Luther-Universität Halle-Wittenberg, 2000
12. G. P. Zhang and W. Hübner, Phys. Rev. Lett. **85**, 3025 (2000)
13. M. Trzeciecki, A. Dähn, and W. Hübner, Phys. Rev. B **60**, 1144 (1999)
14. M. Trzeciecki and W. Hübner, Appl. Phys. B **68**, 473 (1999)
15. M. Fiebig, D. Fröhlich, B. B. Krichevtsov, and R. V. Pisarev, Phys. Rev. Lett. **73**, 2127 (1994)
16. M. Trzeciecki and W. Hübner, Phys. Rev. B **62**, 13888 (2000)
17. to a value close to zero at time t=0, because all the states are nearly equally populated
18. D. P. DiVincenzo and D. Loss, J. Magn. Magn. Mat. **200**, 202 (1999)
19. T. Moos, "Elektronische Theorie für den Ursprung der magnetischen Anisotropieenergie von Fe- und Ni-Monolagen", MSc Thesis, Free University Berlin (1995)